The importance of occupancy rather than affinity of CaVß subunits for the calcium channel I–II linker in relation to calcium channel function

Adrian J. Butcher, Jérôme Leroy, Mark W. Richards, Wendy S. Pratt and Annette C. Dolphin

J. Physiol. 2006;574;387-398; originally published online Apr 20, 2006;

DOI: 10.1113/jphysiol.2006.109744

The importance of occupancy rather than affinity of $Ca_V\beta$ subunits for the calcium channel I–II linker in relation to calcium channel function

Adrian J. Butcher[1], Jérôme Leroy[1], Mark W. Richards[1,2], Wendy S. Pratt[1] and Annette C. Dolphin[1]

[1]*Laboratory of Cellular and Molecular Neuroscience, Department of Pharmacology, University College London, London, UK*
[2]*School of Crystallography, Birkbeck College, London, UK*

The $Ca_V\beta$ subunits of voltage-gated calcium channels regulate the trafficking and biophysical properties of these channels. We have taken advantage of mutations in the tyrosine residue within the alpha interaction domain (AID) in the I–II linker of $Ca_V2.2$ which reduce, but do not abolish, the binding of β1b to the AID of $Ca_V2.2$. We have found that the mutation Y388S decreased the affinity of $Ca_V\beta$1b binding to the $Ca_V2.2$ I–II linker from 14 to 329 nM. However, the Y388S mutation had no effect on current density and cell surface expression of $Ca_V2.2/\alpha2\delta$-2/β1b channels expressed in human embryonic kidney tsA-201 cells, when equivalent proportions of cDNA were used. Furthermore, despite the 24-fold reduced affinity of $Ca_V\beta$1b for the Y388S I–II linker of $Ca_V2.2$, all the key features of modulation as well as trafficking by $Ca_V\beta$ subunits remained intact. This is in contrast to the much more marked effect of the W391A mutation, which abolished interaction with the $Ca_V2.2$ I–II linker, and very markedly affected the trafficking of the channels. However, using the *Xenopus* oocyte expression system, where expression levels can be accurately titrated, when $Ca_V\beta$1b cDNA was diluted 50-fold, all evidence of interaction with $Ca_V2.2$ Y388S was lost, although wild-type $Ca_V2.2$ was still normally modulated by the reduced concentration of β1b. These results indicate that high affinity interaction with the α1 subunit is not necessary for any of the modulatory effects of $Ca_V\beta$ subunits, but occupancy of the interaction site is important, and this will occur, despite the reduced affinity, if the $Ca_V\beta$ subunit is present in sufficient excess.

(Resubmitted 15 March 2006; accepted after revision 13 April 2006; first published online 20 April 2006)
Corresponding author A. C. Dolphin: Laboratory of Cellular and Molecular Neuroscience, Department of Pharmacology, Andrew Huxley Building, University College London, Gower Street, London, WC1E 6BT, UK. Email: a.dolphin@ucl.ac.uk

Voltage-gated calcium (Ca_V) channels are key components of all excitable cells. Three families of voltage-gated calcium channels have been identified, Ca_V1–3. The Ca_V1 and Ca_V2 classes are both high-voltage activated (HVA). These channels are heteromultimers composed of the pore-forming $\alpha1$ subunit, associated with auxiliary $Ca_V\beta$ and $\alpha_2\delta$ subunits (Catterall, 2000). $Ca_V\beta$ subunits are crucial for normal HVA channel function (for review see Dolphin, 2003), since they are required for the expression of functional channels at the plasma membrane (Bichet *et al.* 2000), and modulate their biophysical properties (for review see Dolphin, 2003). The Ca_V2 family calcium channels are inhibited by $G\beta\gamma$ dimers (Herlitze *et al.* 1996; Ikeda, 1996) which is the main mechanism of presynaptic inhibition by G-protein-coupled receptors (GPCRs). $Ca_V\beta$ subunits promote the voltage dependence of modulation of $Ca_V2.2$ calcium channels by $G\beta\gamma$ dimers, although the mechanism involved remains unclear (Meir *et al.* 2000; Canti *et al.* 2001; Leroy *et al.* 2005).

We have previously investigated the role of $Ca_V\beta$ subunits in the plasma membrane expression and modulation of $Ca_V2.2$ calcium channels, by mutating the tryptophan (W391 in $Ca_V2.2$) that is conserved in the AID sequence of all Ca_V1 and 2 channels. This sequence is QQIERELNG**Y**LE**W**IFKAE in $Ca_V2.2$. This tryptophan has been shown both by the original study that identified the AID motif and by the recent structural studies to be key to the interaction between $Ca_V\beta$ subunits and the AID (Pragnell *et al.* 1994; Chen *et al.* 2004; Opatowsky *et al.* 2004; Van Petegem *et al.* 2004). Our results showed that the W391A mutation reduced the binding of β1b to the I–II linker by at least 1000-fold, prevented the enhancement of functional expression of $Ca_V2.2$ by $Ca_V\beta$1b, and also prevented modulation of the biophysical properties of

DOI: 10.1113/jphysiol.2006.109744

$Ca_V2.2$ by this subunit. In addition, although the G-protein modulation of $Ca_V2.2$ W391A was present, it was not voltage dependent (Leroy *et al.* 2005).

We have now investigated the role of the AID tyrosine Y388 in the role of $Ca_V\beta$ subunits and in G protein modulation, since the crystal structure showed the W and Y to form a hairpin arrangement with their aromatic rings stacked together (Chen *et al.* 2004; Opatowsky *et al.* 2004; Van Petegem *et al.* 2004). The Y residue has previously been described as essential for $Ca_V\beta$ binding to the AID and for functional expression (Pragnell *et al.* 1994; Witcher *et al.* 1995). However, a subsequent study disputed the importance of this residue in β subunit-induced modulation of $Ca_V1.2$ currents (Gerster *et al.* 1999), and its role remains open to question. Since in our previous study, measurement of $Ca_V\beta$ binding to the I–II linker by surface plasmon resonance correlated extremely well with the maximum conductance (G_{max}) values for $Ca_V2.2$ currents and with cell surface biotinylation for the W391A mutation (Leroy *et al.* 2005), we performed similar studies following mutation of Y388. Our results allow us to conclude that there is no requirement for high affinity binding of $Ca_V\beta$ to the AID, since this is reduced 24-fold by the mutation Y388S. However, occupancy of the site is a key factor, since reducing the concentration of β1b by 50-fold relative to $Ca_V2.2$ Y388S removed all influence of β1b on this channel, whereas the wild-type $Ca_V2.2$ was still modulated at this concentration of β1b.

Methods

Materials

The cDNAs used in this study were $Ca_V2.2$ (D14157), $Ca_V\beta$1b (X61394), $\alpha2\delta$-2 (Barclay *et al.* 2001) and D_2 dopamine receptor (X17458). The green fluorescent protein (GFP-mut3b, U73901) was used to identify transfected tsA-201 cells. All cDNAs were subcloned in pMT_2.

Construction, expression and purification of proteins

$Ca_V2.2$ Y388S was generated using standard molecular biological methods. The Y388S, Y388F and W391A mutations were introduced into $Ca_V2.2$ I–II loop in pGEX2T (Bell *et al.* 2001) (GST $Ca_V2.2$ I–II loop) by site-directed mutagenesis using standard molecular biological methods. The resulting mutated I–II linkers and the wild-type linker were subcloned into pETM6T1 (gift from Dr A. Okorokov, UCL), which encodes an N-terminal NusA-tag and a His-tag, using *Bam*H I and *Eco*R I, generating NusA $Ca_v2.2$ I–II loop fusion proteins.

NusA $Ca_v2.2$ I–II loop fusion proteins were expressed in BL21(DE3) codon plus (RIL) *E. coli* in 1 litre cultures of LB medium containing 30 μg ml^{-1} kanamycin, 34 μg ml^{-1} chloramphenicol and 1% (w/v) glucose. Cultures were grown to optical density 0.6 at 560 nm and induced at 20°C for 4 h using 0.1 mM isopropyl-β-D-thiogalactopyranoside. For protein purification, cells were lysed by sonication in buffer A (20 mM Hepes pH 8.0, 150 mM NaCl, 1 mM DTT, 20 mM imidazole) containing protease inhibitors (Complete EDTA-free, Roche Diagnostics, Lewes, UK). The lysate was cleared by centrifugation at 20 000 *g* for 20 min and the resulting pellet was washed once with buffer A. The pellet was resuspended in buffer A containing 1.5% CHAPS and incubated for 1 h at 4°C. After centrifugation at 20 000 *g* for 20 min the supernatant was diluted 1 : 1 with buffer A and applied to 1 ml Ni–NTA resin (Qiagen, Crawley, West Sussex, UK) equilibrated with buffer B (buffer A containing 0.5% CHAPS). The column was washed with 25 volumes buffer B before proteins were eluted with 4 volumes buffer B containing 350 mM imidazole. Eluted proteins were analysed by SDS-PAGE followed by Coomassie blue staining. C-terminally His-tagged $Ca_v\beta$1b ($Ca_v\beta$1b-H6C) was expressed and purified as described by Bell *et al.* (2001).

Surface plasmon resonance

Assays were performed using a BIAcore 2000 (Biacore AB, Uppsala, Sweden) at 25°C using running buffer (20 mM Hepes, pH 7.5, 150 mM NaCl, 0.1% CHAPS). NusA fusion proteins and NusA only were immobilized directly onto the surface of a CM5 sensor chip. Using a 1 : 1 mixture of 400 mM 1-ethyl-3-[3-dimethyl-aminopropyl]carbodiimide hydrochloride and 100 mM *N*-hydroxysuccinimide to activate the chip surface, 2000 reference units (RU) of NusA I–II loop fusions and the molar equivalent of NusA were immobilized. $Ca_v\beta$1b-H6C was dialysed against running buffer and diluted to the required concentrations in running buffer. These samples were applied for 5 min at a flow rate of 50 μl min^{-1} over all flow cells and each injection was followed by a 5 min dissociation phase. The sensor chip surface was regenerated between injections by the application of 30 μl of 20 mM glycine pH 2.2 at 10 μl min^{-1}. Sensorgrams were processed using the BIAevaluation 3.0 software (Biacore AB). Sensorgrams recorded from the flow cells containing NusA $Ca_v2.2$ I–II loop, either wild-type, Y388S, or Y388F were corrected for passive refractive index changes and for non-specific interactions by subtraction of the corresponding sensorgram recorded from the flow cell containing NusA only. Sensorgrams were analysed using Biacore kinetic analysis software using a model of 1 : 1 interaction. In addition, the maximum responses for the $Ca_v2.2$ I–II linker and both mutants after 250 s of sample injection were plotted against $Ca_v\beta$ concentration. The resulting curves were analysed by

fitting a rectangular hyperbola, using Origin 7 (Microcal Software, Northhampton, MA, USA), and the affinity constant K_D was estimated. The dissociation phase of the sensorgrams was also fitted to a single exponential, to determine the dissociation rate, k_{off}.

Cell culture and heterologous expression

The tsA-201 cells were cultured in a medium consisting of Dulbecco's modified Eagle's medium, 10% fetal bovine serum, and 1% non-essential amino acids. The cDNAs (all at 1 μg μl^{-1}) for $Ca_V\alpha1$ subunits, $Ca_V\beta$, $\alpha_2\delta$-2, D_2 dopamine receptor and GFP (when used as a reporter of transfected cells) were mixed in a ratio of 3 : 2 : 2 : 2 : 0.4. The cells were transfected using Fugene6 (Roche Diagnostics, Lewes, UK; DNA/Fugene6 ratio of 2 μg in 3 μl).

Cell surface biotinylation and Western blotting

Cell surface biotinylation experiments were carried out as described in Leroy *et al.* (2005). For Western blotting, samples (10 μg) from tsA-201 whole-cell lysates from biotinylation experiments (see above) were separated by SDS-PAGE on 4–12% Tris-glycine gels and then transferred to polyvinylidene fluoride membranes. Immunodetection was performed with antibodies to the $Ca_v2.2$ II–III linker as previously described (Raghib *et al.* 2001).

Whole-cell patch clamp in tsA-201 cells

The tsA-201 cells were replated at low density on 35 mm tissue culture dishes on the day of recording. Whole-cell patch-clamp recordings were performed at room temperature (22–24°C). Only fluorescent cells expressing GFP were used for recording. The single cells were voltage clamped using an Axopatch 200B patch-clamp amplifier (Axon Instruments, Inc., Union City, CA, USA). The electrode potential was adjusted to give zero current between pipette and external solution before the cells were attached. The cell capacitance varied from 10 to 40 pF. Patch pipettes were filled with a solution containing (mM): 140 caesium aspartate, 5 EGTA, 2 $MgCl_2$, 0.1 $CaCl_2$, 2 K_2ATP, 10 Hepes, titrated to pH 7.2 with CsOH (310 mosmol l^{-1}), with a resistance of 2–3 MΩ. The external solution contained (mM) 150 tetraethylammonium (TEA) bromide, 3 KCl, 1.0 $NaHCO_3$, 1.0 $MgCl_2$, 10 Hepes, 4 glucose, 10 $BaCl_2$, pH adjusted to 7.4 with Tris-base (320 mosmol l^{-1}). The pipette and cell capacitance, as well as the series resistance, were compensated by 80%. Leak and residual capacitance current were subtracted using a *P*/4 protocol. Data were filtered at 2 kHz and digitized at 5–10 kHz. The holding potential was −100 mV, and pulses were delivered every 10 s.

Two-electrode voltage clamp in *Xenopus* oocytes

Xenopus laevis females were killed by non-recovery anaesthesia in accordance with Schedule 1 to the Animals (Scientific Procedures) Act, 1986. Oocytes were then surgically removed and defolliculated by treatment with 1.5 mg ml^{-1} collagenase type Ia in a Ca^{2+}-free ND96 saline containing (mM): 96 NaCl, 2 KCl, 1 $MgCl_2$, 5 Hepes, pH adjusted to 7.4 with NaOH, for 2 h at 18°C. Ten nanolitres of cDNAs (1 ng nl^{-1}) were injected into the nuclei of stage V and VI oocytes. Injected oocytes were incubated at 18°C for 3–7 days in ND96 saline (as above plus 1 mM $CaCl_2$) supplemented with 100 μg ml^{-1} penicillin and 100 i.u. ml^{-1} streptomycin (Life Technologies, Gaithersburg, MD, USA). Further details have been previously described (Canti *et al.* 2001).

Whole-cell recordings from oocytes were performed in the two-electrode voltage-clamp configuration under continuous superfusion of a chloride-free solution containing (mM): 10 $Ba(OH)_2$, 50 NaOH, 10 TEA-OH, 2 CsOH, 5 Hepes (pH 7.4 with methanesulphonic acid). The oocytes were injected with 30–40 nl of a 100 mM solution of K_3-1,2-bis(aminophenoxy)ethane-*N*,*N*,*N*′,*N*′-tetra-acetic acid (BAPTA) to suppress endogenous Ca^{2+}-activated Cl^- currents. Electrodes contained 3 M KCl and had resistances of 0.3–1.5 MΩ. The holding potential was −100 mV in all cases. The currents were amplified and low-pass filtered at 1 kHz by means of a Geneclamp 500 amplifier (Axon Instruments, Burlingame, CA, USA), digitized through a Digidata 1200 interface (Axon Instruments). All experiments were performed at 18–20°C.

Electrophysiological data analysis

Current amplitude was measured 10 ms after the onset of the test pulse, and the average over a 2 ms period was calculated and used for subsequent analysis. The current density–voltage (*I*–*V*) relationships were fitted with a modified Boltzmann equation as follows: $I = G_{max}(V - V_{rev})/(1 + \exp(-(V - V_{50,act})/k))$ where I is the current density (in pA pF^{-1}), G_{max} is the maximum conductance (in nS pF^{-1}), V_{rev} is the reversal potential, $V_{50,act}$ is the midpoint voltage for current activation, and k is the slope factor. Steady-state inactivation properties were measured by applying 5 s pulses from −120 to +20 mV in 10 mV increments, followed by a 11 ms repolarization to −100 mV before the 100 ms test pulse to +20 mV. Steady-state inactivation and activation data were fitted with a single Boltzmann equation of the form: $I/I_{max} = (A_1 - A_2)/[1 + \exp((V - V_{50,inact})/k)] + A_2$, where I_{max} is the maximal current, $V_{50,inact}$ is the

half-maximal voltage for current inactivation. For the steady-state inactivation, A_1 and A_2 represent the total and non-inactivating current, respectively. Inactivation kinetics of the currents were estimated by fitting the decaying part of the current traces with the equation: $I(t) = C + A\exp(-(t - t_0)/\tau_{\text{inact}})$ where t_0 is zero time, C the fraction of non-inactivating current, A the relative amplitude of the exponential, and τ_{inact}, its time constant. Activation kinetics were estimated by fitting the activation phase of the current with either a single or a double exponential. Analysis was performed using pCLAMP6 and Origin 7. Data are expressed as mean ± S.E.M. of the number of replicates *n*. Error bars indicate standard errors of multiple determinations. Statistical significance was analysed using Student's paired or unpaired *t* test (as appropriate).

Results

Mutation of Y388S in the I–II linker of $Ca_V2.2$ reduces its affinity for the $Ca_V\beta$1b subunit

The amino acid Y388 in $Ca_V2.2$ is conserved in the AID sequence of all HVA calcium channels (Dolphin, 2003; Richards *et al.* 2004) and has been previously described to be crucial for the binding of the $Ca_V\beta$ ancillary subunits to HVA calcium channels (Pragnell *et al.* 1994; Witcher *et al.* 1995; De Waard *et al.* 1996). The recent structural analysis of the interaction of $Ca_V\beta$ subunits with the $Ca_V1.2$ I–II linker showed that the aromatic ring of the Y side chain is stacked with the side chain of the W residue and deeply embedded in the AID binding groove in $Ca_V\beta$ (Chen *et al.* 2004; Opatowsky *et al.* 2004; Van Petegem *et al.* 2004).

We first examined by surface plasmon resonance analysis whether mutation of Y388 to either F or S in the AID of $Ca_V2.2$ affected the binding of $Ca_V\beta$1b to the I–II linker of $Ca_V2.2$. In these experiments, NusA fusion proteins corresponding to the entire I–II linker, including the AID of $Ca_V2.2$, $Ca_V2.2$ Y388S, $Ca_V2.2$ Y388F or NusA alone as control (Fig. 1*A*), were immobilized chemically onto individual flow cells of a CM5 dextran sensor chip. $Ca_V\beta$ subunit solutions (20–1000 nM) were perfused over all flow cells. No concentration-dependent binding of the $Ca_V\beta$ subunits to the control NusA fusion protein was detected (data not shown). $Ca_V\beta$1b exhibited specific binding to the full-length I–II linker of $Ca_V2.2$ (Fig. 1*B*). Significant binding of $Ca_V\beta$1b was also observed to both the Y388F and Y388S mutant I–II linkers (Fig. 1*C* and *D*).

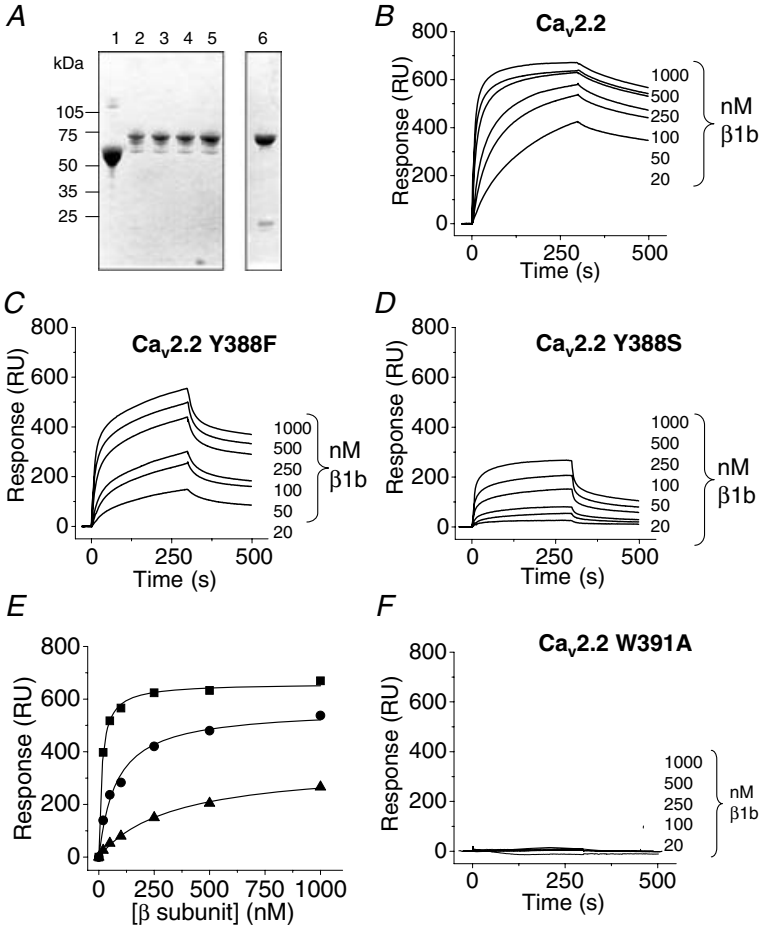

Figure 1. The Y388F and Y388S mutant I–II linkers of $Ca_V2.2$ bind to $Ca_V\beta$1b with reduced affinity
A, Coomassie blue-stained SDS-PAGE gel showing the purity of the wild-type and mutant NusA fusion proteins and the $Ca_V\beta$1b subunit used in surface plasmon resonance analysis. NusA only (lane 1), $Ca_V2.2$ I–II loop (lane 2), $Ca_V2.2$ Y388F (lane 3), $Ca_V2.2$ Y388S (lane 4), $Ca_V2.2$ W391A (lane 5) and $Ca_V\beta$1b (lane 6). Molecular weight markers are indicated. *B–D*, representative Biacore sensorgrams showing interactions between $Ca_V\beta$1b (20–1000 nM as indicated) with NusA I–II loop fusion proteins from $Ca_V2.2$ (*B*), $Ca_V2.2$ Y388F (*C*) and $Ca_V2.2$ Y388S (*D*). K_D values determined from the Biacore analysis software, assuming a 1 : 1 interaction, were 10.5, 64 and 200 nM, respectively, very similar to those determined from panel *E*. *E*, plot showing relationship between response at 250 s after β1b injection for the NusA $Ca_V2.2$ wild-type I–II linker (■), $Ca_V2.2$ Y388F I–II linker (●) and $Ca_V2.2$ Y388S I–II linker (▲) and $Ca_V\beta$1b concentration. Curves were fitted using a rectangular hyperbola function, and the K_D values determined to be 13.7, 78.0 and 329 nM, respectively. *F*, representative Biacore sensorgrams showing negligible interaction between NusA $Ca_V2.2$ W391A I–II linker and $Ca_V\beta$1b at concentrations up to 1000 nM.

The dissociation constant (K_D) for $Ca_V\beta$1b binding to the I–II linker of Ca_V2.2 was calculated to be 13.7 nM for β1b binding to the wild-type I–II linker, and 78 and 329 nM for the Y388F and Y388S mutant I–II linkers, respectively, representing a 5.7-fold and a 24-fold reduction compared to the wild-type I–II linker (Fig. 1*E*). In contrast, negligible binding of the $Ca_V\beta$1b subunit to the Ca_V2.2 W391A I–II linker was detected, and thus the K_D values could not be determined (Fig. 1*F*), as we have previously shown for a GST fusion protein with a I–II linker construct truncated immediately after the AID sequence (Leroy *et al.* 2005). These results refine, rather than contradict, the findings of previous studies which indicated that mutation of Y to S in the AID sequence of other Ca_V channels abrogated $Ca_V\beta$ subunit binding (Pragnell *et al.* 1994; Witcher *et al.* 1995; De Waard *et al.* 1996; Berrou *et al.* 2002), since all previous studies have used non-quantitative overlay or pull-down assays, where low affinity interactions may easily be missed.

Single exponential fits were made to the dissociation phases of the sensorgrams, and the dissociation rate constants (k_{off}) of 20 nM $Ca_V\beta$1b from the I–II linkers of Ca_V2.2, Ca_V2.2 Y388F and Ca_V2.2 Y388S were calculated to be $8.1 \times 10^{-3}\ s^{-1}$, $16 \times 10^{-3}\ s^{-1}$ and $39 \times 10^{-3}\ s^{-1}$, respectively. As expected, there was little variation in the dissociation rates for each mutant across the range of $Ca_V\beta$1b concentrations used in these experiments. Our findings highlight the contributions made by the hydroxyl group and phenyl group of this Y residue to the high affinity interaction between AID and $Ca_V\beta$.

The effect of Y388S mutation on the functional expression of Ca_V2.2 calcium channels at the plasma membrane

Since the mutation of Y388S reduced the affinity for $Ca_V\beta$1b to a greater extent than the Y388F mutation, we used the Y388S mutation in full length Ca_V2.2 for further functional studies. We coexpressed full length Ca_V2.2 Y388S or wild-type Ca_V2.2, together with accessory $Ca_V\beta$1b and $\alpha_2\delta$-2 subunits and compared the biophysical properties of the wild-type and mutated channels. Surprisingly, and unlike the W391 mutant of Ca_V2.2 that we studied recently (Leroy *et al.* 2005), there was no significant difference in G_{max} determined from the current–voltage (I–V) relationships between wild-type Ca_V2.2 and Ca_V2.2 Y388S (Fig. 2*A*). The G_{max} of Ca_V2.2

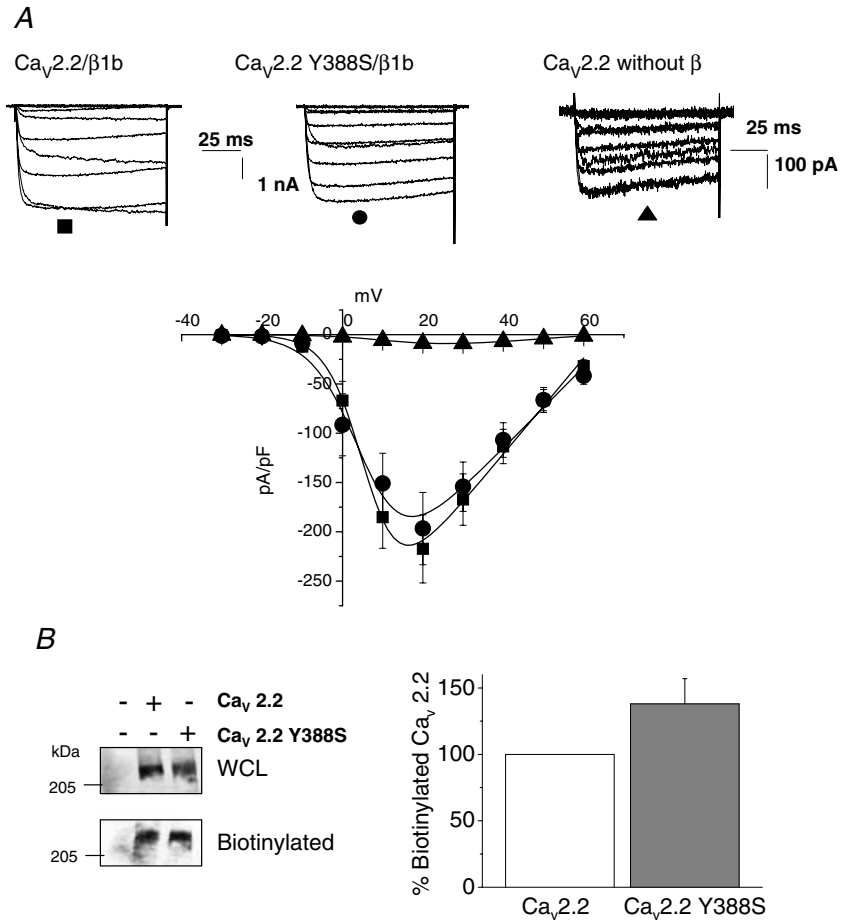

Figure 2. Role of $Ca_V\beta$ subunits in plasma membrane expression of Ca_V2.2
A: upper panel, superposition of representative current traces for the subunit combinations indicated, recorded during 100 ms, 10 mV steps from −30 mV to +60 mV, from a holding potential of −100 mV. Same scale bars for the left and centre panels; lower panel, *I–V* relationships (mean ± S.E.M.) for Ca_V2.2/$\alpha_2\delta$-2 coexpressed with $Ca_V\beta$1b (■, $n = 29$) or without a $Ca_V\beta$ subunit (▲, $n = 21$), compared to the *I–V* relationship for Ca_V2.2 Y388S/$\alpha_2\delta$-2/$Ca_V\beta$1b (●, $n = 17$). The mean data are fitted with a modified Boltzmann function (see Methods). *B*, cell surface expression of either Ca_V2.2 or Ca_V2.2 Y388S expressed with $\alpha_2\delta$-2 and $Ca_V\beta$1b. Left panel, total expression of Ca_V2.2 in whole-cell lysate (WCL) is shown by Western blot in the upper row, and biotinylated Ca_V2.2, in the streptavidin agarose precipitate, is shown in the lower row. Cells were transfected with empty vector (lane 1), Ca_V2.2/$\alpha_2\delta$-2/β1b (lane 2) or Ca_V2.2 Y388S/$\alpha_2\delta$-2/β1b (lane 3). Right panel, bar chart showing quantification of the mean amount of Ca_V2.2 Y388S expressed at the plasma membrane when coexpressed with β1b (grey bar), given as a percentage of the amount of Ca_V2.2 expressed under the same conditions (white bar). Data are mean ± S.E.M. of 3 independent experiments. The cell surface expression of Ca_V2.2 was increased slightly by the Y388S mutation in all three experiments.

Y388S was 97.5 ± 16% ($n = 17$) of that found for the $Ca_V2.2/\beta1b/\alpha_2\delta$-2 combination when coexpressed with $\beta1b$. Thus, the auxiliary $\beta1b$ subunit was still able to significantly increase the G_{max} of $Ca_V2.2$ Y388S when compared with either the wild-type $Ca_V2.2$ expressed alone (Fig. 2*A*) or with the $Ca_V2.2$ Y388S/$\alpha_2\delta$-2 ($n = 4$, data not shown). In the transfection system used, the over-expression of $Ca_V\beta$ may mean that the AID site is constantly occupied despite the 24-fold lower affinity of the Y388S mutant AID. Thus the high affinity interaction of $Ca_V\beta$, previously suggested to be essential for the trafficking to the plasma membrane may not be necessary, but occupancy of the site may be the most important factor.

We then used a cell surface biotinylation assay to assess biochemically whether there was an alteration in the amount of channel protein present at the surface of the tsA-201 cells transfected with $Ca_V2.2$ Y388S and a $Ca_V\beta$ subunit, compared with the wild-type $Ca_V2.2/Ca_V\beta$ combination. The $Ca_V2.2$ Y388S mutation had no effect upon the total expression compared to wild-type $Ca_V2.2$, whereas the amount of biotinylated $Ca_V2.2$ Y388S channels at the plasma membrane was non-significantly elevated by 38 ± 19% ($n = 3$; Fig. 2*B*). Together these results show that the Y388S mutation in $Ca_V2.2$ has no detrimental effect upon the trafficking and functional expression of $Ca_V2.2$ channels. This implies that the $Ca_V\beta1b$ can still associate with, and effectively exert its trafficking effects on, the Y388S mutant channel even though the affinity of the Y388S AID/$Ca_V\beta$ interaction is reduced over 20-fold. This is in agreement with previous studies which have shown little or no effect of a Y to S mutation in AID of $Ca_V1.1$ or $Ca_V2.3$ channels on functional expression (Neuhuber *et al.* 1998; Berrou *et al.* 2002). However, it is in contrast to the earlier studies that identified the key amino acids responsible for $Ca_V\beta$ subunit binding to the AID and showed that Y was one of the main amino acids whose mutation markedly reduced functional expression (Pragnell *et al.* 1994; De Waard *et al.* 1996).

Biophysical properties of $Ca_V2.2$ Y388S expressed with $Ca_V\beta1b$ are similar to those of $Ca_V2.2/\beta1b$

As well as having effects on trafficking, $Ca_V\beta1b$ is known to promote the activation of HVA calcium channels at more negative potentials (for review see Dolphin, 2003). In a previous study, we have estimated that the effects of $Ca_V\beta$ subunits on the voltage-dependent properties of the channels occurred with an approximately 7-fold lower affinity than the effects on trafficking (Canti *et al.* 2001). It is therefore possible that $Ca_V2.2$ Y388S would be trafficked to the plasma membrane by $Ca_V\beta1b$, despite its reduced affinity, but would lose any interaction following trafficking. However, from the *I–V* relationships, the $Ca_V2.2$ Y388S had a similar V_{50} for activation (+5.5 ± 1.5 mV; $n = 17$) to wild-type $Ca_V2.2$ in the presence of $\beta1b$ (+6.0 ± 0.6 mV; $n = 29$), which were both significantly less positive compared with V_{50} for activation for the wild-type $Ca_V2.2$ expressed alone (+14.4 ± 0.4 mV; $n = 21$, $P < 0.05$) (Fig. 2*A*). This indicates that the reduction in affinity conferred by the Y388S mutation was insufficient to alter the effect of $Ca_V\beta1b$ on the voltage dependence of activation of the channel, and this mutant channel behaved like the wild-type $Ca_V2.2$, expressed with a $Ca_V\beta1b$ subunit.

Another important feature of $Ca_V\beta1$, $\beta3$ and $\beta4$ subunits is that they hyperpolarize the steady-state inactivation curves of $Ca_V2.2$, as well as other HVA calcium channels (Bogdanov *et al.* 2000). The potential for half-inactivation ($V_{50,inact}$) was −45.4 ± 0.4 mV ($n = 25$) for $Ca_V2.2$ expressed with $Ca_V\beta1b$ (Fig. 3), representing a −15 mV shift compared to $Ca_V2.2$ expressed in the absence of a β subunit. Again, we found no significant effect on the steady-state inactivation for $Ca_V2.2$ Y388S/$\beta1b$, as this was superimposed on that of $Ca_V2.2$ expressed with $Ca_V\beta1b$ (Fig. 3*A* and *B*).

$Ca_V\beta$ subunits are known to modulate not only the voltage dependence of the inactivation of calcium channels, but also the kinetics of current decay (for review see Dolphin, 2003). The time constant of inactivation (τ_{inact}) of the $Ca_V2.2$ Y388S/$\beta1b$ current recorded during 800 ms pulses at +20 mV (550 ± 161 ms; $n = 14$) was the same as that of the wild-type $Ca_V2.2/\beta1b$ combination (557 ± 88 ms; $n = 14$) (Fig. 3*C*). Altogether these results indicate that $Ca_V2.2$ Y388S is normally regulated by $Ca_V\beta1b$ in the plasma membrane.

$Ca_V2.2$ Y388S channels show normal voltage-dependent modulation by G-protein activation

To investigate the importance of the Y388 residue for the modulation by G-proteins of $Ca_V2.2$ calcium channels, the wild-type or mutant $Ca_V2.2$, $Ca_V\beta1b$, $\alpha_2\delta$-2 combination was coexpressed with a D_2 dopamine receptor, and the receptor was activated with 100 nM quinpirole, which is a maximal concentration of this agonist. Figure 4*A* shows representative currents obtained before and during application of quinpirole, both before (P1) and immediately after (P2) a 100 ms prepulse to +100 mV. As previously observed (Leroy *et al.* 2005), the currents measured at +10 mV were inhibited by quinpirole by 64.2 ± 4.0% for the wild-type channel ($n = 29$; Fig. 4*B*). The P2/P1 ratio obtained from traces such as those represented in Fig. 4*A* reflects the voltage-dependent removal of G-protein inhibition. A value of 2.2 ± 0.1 ($n = 29$) was obtained for P2/P1 at +10 mV for the wild-type channel expressed with $Ca_V\beta1b$ (Fig. 4*C*).

For the $Ca_V2.2$ Y388S/$\beta1b$ currents, inhibition by quinpirole was 63.0 ± 8.5% at +10 mV ($n = 17$; Fig. 4*A*

and *B*), and it showed similar voltage dependence to the wild-type currents, the P2/P1 ratio being 2.3 ± 0.2 at +10 mV ($n = 17$), very similar to that for $Ca_V2.2/\beta1b$ ($P < 0.01$, Fig. 4*C*).

We have shown previously that lowering the concentration of expressed $Ca_V\beta$ subunits leads to a slower rate of facilitation of the G-protein-modulated current, with two components of facilitation being present at intermediate $Ca_V\beta$ concentrations (Canti *et al.* 2001). Thus a reduction in affinity of $Ca_V\beta$ for the $Ca_V2.2$ Y388S channel might be manifested by a reduction in facilitation rate. We therefore determined the time constants of facilitation (τ_{facil}) by varying the prepulse duration during quinpirole application, and found that the τ_{facil} was very similar for the wild-type $Ca_V2.2$ (10.2 ± 0.7 ms; $n = 11$) and $Ca_V2.2$ Y388S (11.2 ± 0.8 ms; $n = 12$) (Fig. 5).

The interaction between $Ca_V2.2$ Y388S and $Ca_V\beta1b$ is lost when the concentration of $\beta1b$ is reduced

From the foregoing, it is clear that a 24-fold reduction in affinity of $Ca_V\beta1b$ for the $Ca_V2.2$ AID containing the Y388S mutation is insufficient to have any effect on the ability of $\beta1b$ to modulate the channel, by all the parameters we have studied, although we know from the W391A mutation that binding to the AID region is essential for these effects of $\beta1b$ to occur (Leroy *et al.* 2005). We also know from our previous study in *Xenopus* oocytes that the amount of $\beta1b$ expressed when $Ca_V2.2$ and $\beta1b$ cDNAs are injected in an equivalent ratio is at least 30-fold in excess of that required to hyperpolarize the voltage dependence of steady-state inactivation of the entire channel population (Canti *et al.* 2001). We therefore examined the properties of wild-type $Ca_V2.2$ and $Ca_V2.2$ Y388S coexpressed with $\beta1b$ either at a normal cDNA ratio or using 50-fold diluted $\beta1b$ cDNA in *Xenopus* oocytes. For wild-type $Ca_V2.2$, the effects of both concentrations of $\beta1b$ were identical, both in terms of peak current amplitude at +10 mV (Fig. 6*A*), and in terms of hyperpolarization of the steady-state inactivation (Fig. 6*B*). For the steady-state inactivation, the $V_{50,inact}$ was -51.0 ± 1.1 mV for $Ca_V2.2/\beta1b$ injected in a standard ratio ($n = 10$) and -46.8 ± 1.3 mV for $Ca_V2.2/\beta1b$ using 50-fold-diluted $\beta1b$ cDNA ($n = 7$). This result is in

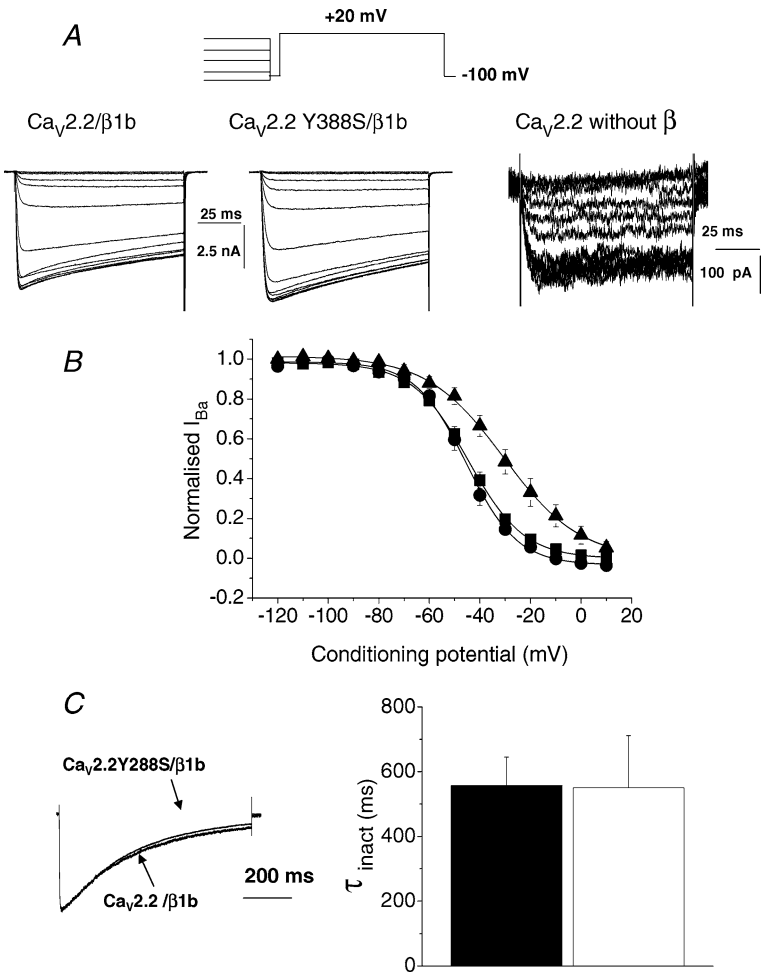

Figure 3. Inactivation properties of $Ca_V2.2$ and $Ca_V2.2$ Y388S coexpressed with $Ca_V\beta1b$
A, voltage protocol and representative current traces to illustrate steady-state inactivation protocols. Inward Ba^{2+} currents were recorded after conditioning pulses of 5 s duration, applied from a holding potential of −100 mV in 10 mV steps between −120 and +10 mV, followed by a 50 ms test pulse to +20 mV. Same scale bars for the left and centre panels. *B*, voltage dependence of steady-state inactivation for $Ca_V2.2/\alpha_2\delta$-2 coexpressed with $Ca_V\beta1b$ (■), without any $Ca_V\beta$ subunits (▲) or $Ca_V2.2$ Y388S/$\alpha_2\delta$-2 expressed with $Ca_V\beta1b$ (●). The normalized data, obtained from recordings such as those shown in the upper panel, are plotted against the conditioning pulse ($n = 10$–25). The mean data are fitted with a Boltzmann function, whose $V_{50,inact}$ values are given in the text. *C*, currents were recorded at +20 mV for 800 ms, and normalized to the peak current before averaging. Left panel, mean normalized current traces for $Ca_V2.2$ Y388S/$\alpha_2\delta$-2/$\beta1b$ and wild-type $Ca_V2.2/\alpha_2\delta$-2/$\beta1b$ combination. Right panel, mean τ_{inact} data for wild-type $Ca_V2.2/\alpha_2\delta$-2/$\beta1b$ (filled bar, $n = 14$) and $Ca_V2.2$ Y388S/$\alpha_2\delta$-2/$\beta1b$ (open bar, $n = 14$).

agreement with our previous findings (Canti *et al.* 2001). It can be attributed to the fact that $Ca_V\beta$ subunits, being low molecular weight cytoplasmic proteins, are transcribed and translated more rapidly and are therefore likely to be present in the cytoplasm at much higher concentrations than the concentration of functional transmembrane $Ca_V2.2$ channels at the plasma membrane. However, for $Ca_V2.2$ Y388S there was a clear difference between the effects of the two concentrations of $Ca_V\beta1b$, in that the currents in the presence of the 50-fold diluted $\beta1b$ were significantly reduced by 74% ($P < 0.01$) compared to those in the presence of the standard concentration of $\beta1b$

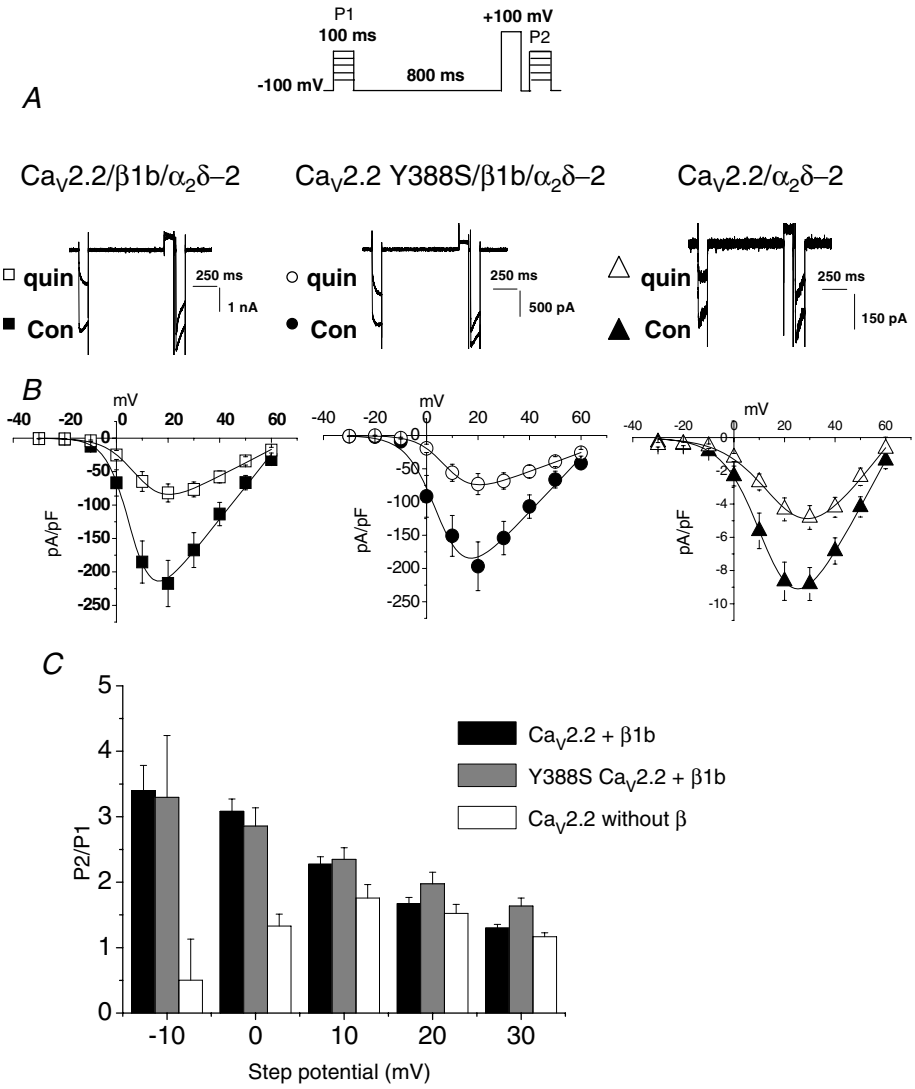

Figure 4. G-protein modulation of $Ca_V2.2$ and $Ca_V2.2$ Y388S currents
A, the pulse protocol used consisted of a 100 ms test pulse (P1) from −30 mV to +60 mV applied from a holding potential of −100 mV. After 800 ms repolarization to −100 mV, a 100 ms prepulse to +100 mV was applied. The cell was repolarized for 20 ms to −100 mV and a second pulse (P2) identical to the first one was applied. Typical current traces obtained with this protocol are represented for $Ca_V2.2$ and $Ca_V2.2$ Y388S coexpressed with $\alpha_2\delta$-2 and $Ca_V\beta1b$, and for $Ca_V2.2$ expressed without a $Ca_V\beta$ subunit. The D_2 dopamine receptor is coexpressed and the upper current traces (depicted by the open symbols) are in the presence of the agonist quinpirole (100 nM). *B*, *I–V* curves, obtained from currents evoked by P1, for the calcium channel combinations shown, obtained before (filled symbols) and during (open symbols) application of 100 nM quinpirole. *I–V* curves for $Ca_V2.2/\alpha_2\delta$-2 coexpressed with $Ca_V\beta1b$ (squares, $n = 29$) or without $\beta1b$ (triangles, $n = 21$) and for $Ca_V2.2$ Y388S/$\alpha_2\delta$-2 coexpressed with $Ca_V\beta1b$ (circles, $n = 17$) are represented. *I–V* curves are fitted with modified Boltzmann functions whose $V_{50,act}$ values are given in the Results. *C*, voltage-dependent facilitation was calculated by dividing the peak current value obtained in P2 by that obtained in P1 at the potentials of −10, 0, +10 +20 and +30 mV, for $Ca_V2.2/\alpha_2\delta$-2 with (black bars, $n = 29$) or without $Ca_V\beta1b$ (white bars, $n = 19$) or for $Ca_V2.2$ Y388S/$\alpha_2\delta$-2 with $Ca_V\beta1b$ (grey bars, $n = 17$) after application of quinpirole.

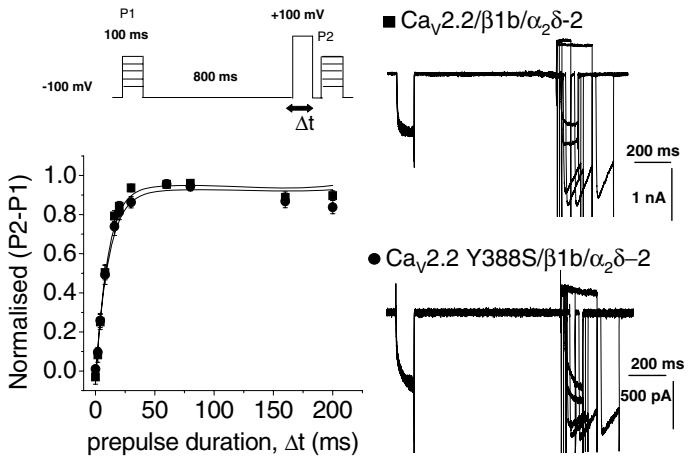

Figure 5. Facilitation rate of G-protein-modulated channels
Left panels, the pulse protocol used to estimate the facilitation rate was similar to the one described in the legend to Fig. 4, but the duration of the prepulse was increased from 0 to 200 ms. The P2/P1 facilitation ratios are given for each prepulse, for $Ca_V2.2$ (■, $n = 11$) and $Ca_V2.2$ Y388S (●, $n = 12$) coexpressed with $Ca_V\beta1b$. Data are fitted with a single exponential, whose time constant (τ_{facil}) is given in the text. Right panels, typical current traces obtained for $Ca_V2.2/\alpha_2\delta$-2 and for $Ca_V2.2$ Y388S/$\alpha_2\delta$-2, both coexpressed with $Ca_V\beta1b$ and the D_2 dopamine receptor, are represented.

(Fig. 6*A*), and the steady-state inactivation became more positive, to the same extent as in the absence of any β subunit (Fig. 6*B*). The $V_{50,inact}$ was -44.9 ± 2.0 mV for $Ca_V2.2$ Y388S/$\beta1b$ injected in the standard ratio ($n = 7$) and -16.5 ± 0.45 mV for $Ca_V2.2$ Y388S/$\beta1b$ injected in the diluted ratio ($n = 10$, $P < 0.001$ compared to the standard ratio). This is very similar to the $V_{50,inact}$ obtained for steady-state inactivation curves of $Ca_V2.2/\alpha_2\delta$-2 currents, which was -18.0 ± 1.5 mV ($n = 10$; Fig. 6*B*). Thus a reduction in the concentration of expressed $Ca_V\beta$ subunits reveals the functional effect of the lower affinity of the $Ca_V2.2$ Y388S I–II linker for $Ca_V\beta$ subunits.

Discussion

$Ca_V\beta$ subunits are membrane-associated guanylate kinase proteins characterized by a guanylate kinase-like (GK) domain that binds to the AID motif in the I–II loop of HVA $Ca_V\alpha1$ subunits (Fig. 1*A*) and a Src homology 3 domain (SH3) (Hanlon *et al.* 1999). The 18 amino acid AID motif contains a conserved W that is crucial for binding $Ca_V\beta$ (Pragnell *et al.* 1994; Berrou *et al.* 2002; Leroy *et al.* 2005), and also a conserved Y three residues proximal to the W. Recent structural data from three groups has provided detailed information about the interaction between the AID–$Ca_V\beta$ complex and confirmed that both W and Y are deeply embedded in the binding groove within the GK of $Ca_V\beta$ (Van Petegem *et al.* 2004; Opatowsky *et al.* 2004; Chen *et al.* 2004). The importance of the Y in $Ca_V\beta$ binding and functional effects is controversial. It was first found that mutation of this Y to S in the AID of $Ca_V2.1$ completely abolished binding to $\beta3$, and almost completely abolished binding to $\beta2a$, whereas the mutation of Y to F appeared to be slightly less effective (Witcher *et al.* 1995). This Y residue was also originally described as being essential for functional expression (Pragnell *et al.* 1994; Witcher *et al.* 1995). However, Berrou *et al.* (2002) found that although no direct binding of the ^{35}S-labelled $Ca_v\beta3$ subunit to a GST $Ca_v2.3$ AID

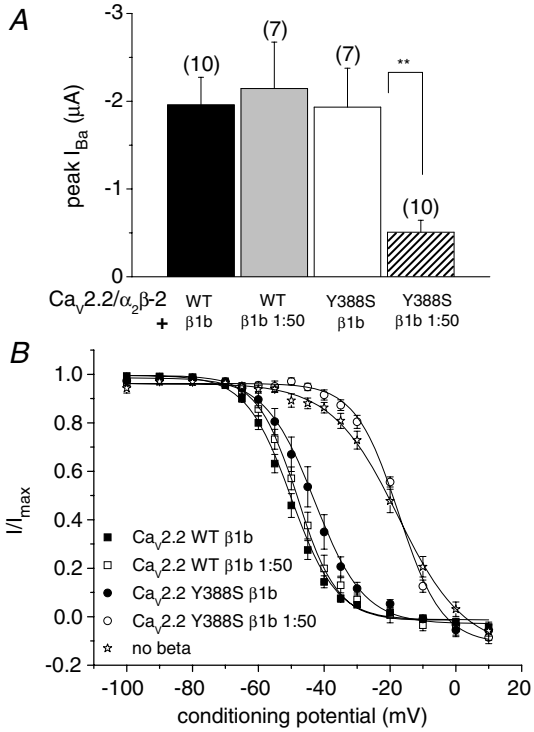

Figure 6. The effect of a 50-fold dilution of β1b on the expression and steady-state inactivation properties of $Ca_V2.2$ and $Ca_V2.2$ Y388S in *Xenopus* oocytes
A, peak current levels at +10 mV of $Ca_V2.2/\alpha_2\delta$-2 coexpressed with $Ca_V\beta1b$ in the standard ratio (black bar, $n = 10$) or with 1 : 50 diluted $\beta1b$ cDNA (grey bar, $n = 7$), or $Ca_V2.2$ Y388S/$\alpha_2\delta$-2 coexpressed with $Ca_V\beta1b$ in the standard ratio (white bar, $n = 7$) or with 1 : 50 diluted $\beta1b$ cDNA (hatched bar, $n = 10$). ** $P < 0.01$, statistically significant compared to the standard ratio of $Ca_V2.2$ Y388S/$Ca_V\beta1b$, using Student's two-tailed *t* test. *B*, voltage dependence of steady-state inactivation of $Ca_V2.2/\alpha_2\delta$-2 coexpressed with $Ca_V\beta1b$ in the standard ratio (■, $n = 10$) or with 1 : 50 diluted $\beta1b$ cDNA (□, $n = 7$), or $Ca_V2.2$ Y388S/$\alpha_2\delta$-2 coexpressed with $Ca_V\beta1b$ in the standard ratio (●, $n = 7$) or with 1 : 50 diluted $\beta1b$ cDNA (○, $n = 10$), and compared to data obtained without any β subunit coexpressed (☆, $n = 10$). The normalized data are plotted against the conditioning potential. The mean data are fitted with a Boltzmann function, whose $V_{50,inact}$ values are given in the text.

containing the Y to S mutation could be detected, $Ca_v2.3$ Y383S was still in part modulated by the $Ca_v\beta3$ subunit when coexpressed in *Xenopus* oocytes. Berrou *et al.* (2005) subsequently found that both conserved and non-conserved mutations in Y383 of $Ca_V2.3$ had little effect on $Ca_V\beta$ modulation of whole-cell currents in *Xenopus* oocytes but the same mutations in an AID peptide almost abolished ^{35}S-labelled $Ca_v\beta3$ binding, using a non-quantitative assay. In addition, Neuhuber *et al.* (1998) found that whilst Y366S mutation in $Ca_V1.1$ appeared to prevent co-localization of $Ca_V1.1$ with $Ca_V\beta1a$ in transfected tsA-201 cells, expression of $Ca_V1.1$ currents was not affected. Similar results were found by the same group for the same Y to S mutation in $Ca_V1.2$, which prevented co-localization of $Ca_V1.2$ with β subunits at the plasma membrane, as determined by immunocytochemistry, but did not affect calcium current expression (Gerster *et al.* 1999). This group concluded that increased incorporation of channels into the plasma membrane is not required for the $Ca_V\beta$-mediated enhancement of functional calcium currents.

Our evidence that β subunits increase the number of $Ca_V2.2$ channels incorporated into the plasma membrane, as determined by cell surface biotinylation (Leroy *et al.* 2005), and that this is reduced by the W391A mutation (Leroy *et al.* 2005) but not by the Y388S mutation (as shown here using the same transfection conditions), are in agreement with the effect of these two mutations on $Ca_V2.2$ current density, although the effect on cell surface incorporation was always less than the overall influence on current density. Our results strongly support the view that both the $Ca_V\beta$-mediated increase in channel number in the plasma membrane, as well as the undisputed effect of $Ca_V\beta$ subunits on channel properties (Neely *et al.* 1993; Gerster *et al.* 1999; Meir *et al.* 2000), both normally contribute to the increase in whole-cell current that is observed. It is likely that previous immunocytochemical results, using intracellular epitopes that require cell permeabilization (Neuhuber *et al.* 1998; Gerster *et al.* 1999), do not allow the distinction between sub- plasma membrane channels, and those that are actually in the membrane, whereas cell surface biotinylation is a more accurate reflection of proteins that are incorporated into the membrane.

Low affinity interactions of different $Ca_V\beta$ subunits with the N- and C-termini of various calcium channels have also been reported (for reviews see Walker & De Waard, 1998; Dolphin, 2003), although in a yeast two-hybrid screen we did not observe any interaction of $Ca_V\beta1b$ with the N- or C-terminus of $Ca_V2.2$, under conditions where the interaction of $Ca_V\beta1b$ with the I–II linker was robust (Raghib *et al.* 2001). Furthermore, it is unlikely that such interactions could be responsible for the effects of $Ca_V\beta$ subunits in the absence of an anchor to the AID region of the I–II linker, since all the effects of $\beta1b$ were abrogated by the W391A mutation (Leroy *et al.* 2005). However, palmitoylated $\beta2a$ was still able to modulate the biophysical properties of $Ca_V2.2$ W391A, indicating that the plasma membrane anchoring afforded by its palmitoylation can substitute for high affinity interaction with the I–II linker (Leroy *et al.* 2005). Thus it seems likely that several other regions of the calcium channel $\alpha1$ subunits are involved in mediating the effects of $Ca_V\beta$ subunits.

Lack of evidence for the binding of $Ca_V\beta$ subunits to additional regions on the I–II linker, apart from the AID

In this study we obtained a similar affinity of $Ca_V\beta1b$ for the full-length $Ca_V2.2$ I–II linker to that which we found previously for a I–II linker construct truncated immediately after the AID (13.8 nM; Leroy *et al.* 2005). If there were an additional binding site, for example for the β subunit SH3 domain, to a site on the I–II linker distal to the AID, as suggested previously (Maltez *et al.* 2005), the combination of two binding sites would lead to the measurement of a higher overall affinity of $Ca_V\beta$ for the full-length I–II linker. Our results, combined with the complete lack of binding of $\beta1b$ to the full-length $Ca_V2.2$ W391A I–II linker, do not provide evidence that there is an additional binding site for other domains of $\beta1b$ on the distal I–II linker of $Ca_V2.2$, in contrast to the previous conclusion (Maltez *et al.* 2005).

The Y388S mutation in the AID of $Ca_V2.2$ appears not to influence the functional effects of $\beta1b$, despite producing a 24-fold reduction in affinity for $\beta1b$ binding to the AID

One of the main effects of $Ca_V\beta$ subunits on HVA calcium channels is to increase current density. Our studies have shown that there are fewer channels present at the cell surface when no $Ca_V\beta$ subunits were coexpressed or when mutated $Ca_V2.2$ W391A channels were cotransfected with a $Ca_V\beta$ (Leroy *et al.* 2005). It has been suggested that a $Ca_V\beta$ bound to the I–II linker may mask an endoplasmic reticulum retention signal present in the I–II linker of HVA calcium channels and favour the trafficking of the channel to the cell surface (Bichet *et al.* 2000). Our previous data suggested that the endogenous $Ca_V\beta3$ that we have identified in tsA-201 cells was responsible for trafficking some wild-type $Ca_V2.2$ to the plasma membrane in the absence of a coexpressed β subunit, and that the markedly reduced affinity of the W391A mutated channel for $Ca_V\beta$ subunits abolished interaction with the endogenous $Ca_V\beta3$ subunits, and thus prevented any trafficking to the plasma membrane (Leroy *et al.* 2005). Our results therefore provided very strong evidence that the binding of a $Ca_V\beta$ subunit to the channel is an essential requirement for the functional expression of $Ca_V2.2$ at the plasma membrane.

In contrast, the markedly reduced affinity of the Y388S AID (from 13.7 to 329 nM) for β1b does not translate into a reduced expression of the channels at the plasma membrane, or any effect on the voltage dependence of activation or inactivation or voltage dependence of G-protein modulation. We have determined previously, from experiments in which varying concentrations of β subunits were expressed together with a constant amount of $Ca_V2.2$ in *Xenopus* oocytes, that there appeared to be two different affinities of β subunits for trafficking the channels (approximately 17 nM for β3) and for hyperpolarizing the steady-state inactivation (about 7-fold lower affinity, approximately 120 nM). However, in *Xenopus* oocytes the concentration of $Ca_V\beta$ subunits obtained following the standard conditions of heterologous expression used in this study was estimated to be far in excess of this, at 2–3 μM (Canti *et al.* 2001). If similar amounts are expressed in the mammalian expression system then it is not surprising that little effect was observed of a 24-fold reduction in the affinity of β1b for the AID. Occupancy would remain very high because of the excess of free $Ca_V\beta$ subunits.

Support is given to this conclusion by our experiments in *Xenopus* oocytes in which dilution of β1b by 50-fold abolished the influence of this $Ca_V\beta$ subunit on the steady-state inactivation of $Ca_V2.2$ Y388S but had no effect on that of wild-type $Ca_V2.2$.

These experiments demonstrate the limitation of coexpression studies in that the concentration of the expressed proteins may be very different, particularly when coexpressing membrane proteins with cytoplasmic proteins, despite the use of similar cDNA concentrations, and in this way they may not mimic the ratios of subunits present *in vivo*. However, the stoichiometry and occupancy of the AID site on endogenous calcium channels by endogenous $Ca_V\beta$ subunits remains an open question to be addressed in the future.

The Y388S mutation in the AID of $Ca_V2.2$ has no effect on G-protein modulation of $Ca_V2.2$ channels

It has been proposed that G-protein modulation of Ca_V2 channels involves competition between $G\beta\gamma$ and $Ca_V\beta$ subunits, with displacement of β subunits being a key step (Bourinet *et al.* 1996; Sandoz *et al.* 2004). Our results do not support this view as, despite the 24-fold reduction in affinity of $Ca_V2.2$ Y388S for β1b, there was no enhancement of G-protein modulation. If there were simple competition between $G\beta\gamma$ and $Ca_V\beta$, then a 24-fold reduction in affinity of the I–II linker for $Ca_V\beta$1b should result in an increased occupancy by $G\beta\gamma$ at the peak of the response to the agonist quinpirole. The present result concurs with our previous results that did not provide evidence for simple competition between $Ca_V\beta$ and $G\beta\gamma$ (Meir *et al.* 2000).

All parameters of G-protein modulation were identical, including the rate of facilitation, which has been interpreted as resulting from the dissociation of $G\beta\gamma$ (Ikeda, 1996; Zamponi & Snutch, 1998). In our previous study we found that the facilitation rate during a +100 mV prepulse was a sensitive measure of changes in $Ca_V\beta$ subunit concentration (Canti *et al.* 2001). It was 20-fold slower in the absence than in the presence of coexpressed $Ca_V\beta$ subunits, and could be resolved into different proportions of fast and slow components in the presence of intermediate concentrations of $Ca_V\beta$ subunits (Canti *et al.* 2001). Our interpretation of these two components was that the fast component represented $G\beta\gamma$ dissociation from channels to which $Ca_V\beta$ was already bound, and the slow rate represented increased $Ca_V\beta$ binding at +100 mV, followed by $G\beta\gamma$ dissociation, since the slow rate depended on $Ca_V\beta$ subunit concentration (Canti *et al.* 2001). In agreement with our previous results, this suggests that $Ca_V\beta$ subunit displacement by $G\beta\gamma$ is not involved in G-protein modulation (Meir *et al.* 2000; Canti *et al.* 2000; Leroy *et al.* 2005), but in contrast the presence of bound β subunits is essential to promote the loss of $G\beta\gamma$ at positive potentials (prepulse facilitation) (Meir *et al.* 2000; Leroy *et al.* 2005).

References

Barclay J, Balaguero N, Mione M, Ackerman SL, Letts VA, Brodbeck J, Canti C, Meir A, Page KM, Kusumi K, PerezReyes E, Lander ES, Frankel WN, Gardiner RM, Dolphin AC & Rees M (2001). Ducky mouse phenotype of epilepsy and ataxia is associated with mutations in the *Cacna2d2* gene and decreased calcium channel current in cerebellar Purkinje cells. *J Neurosci* **21**, 6095–6104.

Bell DC, Butcher AJ, Berrow NS, Page KM, Brust PF, Nesterova A, Stauderman KA, Seabrook GR, Nurnberg B & Dolphin AC (2001). Biophysical properties, pharmacology and modulation of human, neuronal L-type (α1D, $Ca_V1.3$) voltage-dependent calcium currents. *J Neurophysiol* **85**, 816–828.

Berrou L, Klein H, Bernatchez G & Parent L (2002). A specific tryptophan in the I–II linker is a key determinant of beta-subunit binding and modulation in $Ca_V2.3$ calcium channels. *Biophys J* **83**, 1429–1442.

Berrou L, Dodier Y, Rayband A, Tousignant A, Dafi O, Pelletier JN, Parent L (2005). The C-terminal residues in the alpha-interacting domain (AID) helix anchor CaV beta subunit interaction and modulation of CaV2.3 channels. *J Biol Chem* **280**, 494–505.

Bichet D, Cornet V, Geib S, Carlier E, Volsen S, Hoshi T, Mori Y & De Waard M (2000). The I–II loop of the Ca^{2+} channel α1 subunit contains an endoplasmic reticulum retention signal antagonized by the β subunit. *Neuron* **25**, 177–190.

Bogdanov Y, Brice NL, Canti C, Page KM, Li M, Volsen SG & Dolphin AC (2000). Acidic motif responsible for plasma membrane association of the voltage-dependent calcium channel β1b subunit. *Eur J Neurosci* **12**, 894–902.

Bourinet E, Soong TW, Stea A & Snutch TP (1996). Determinants of the G protein-dependent opioid modulation of neuronal calcium channels. *Proc Natl Acad Sci U S A* **93**, 1486–1491.

Canti C, Bogdanov Y & Dolphin AC (2000). Interaction between G proteins and accessory β subunits in the regulation of α1B calcium channels in *Xenopus* oocytes. *J Physiol* **527**, 419–432.

Canti C, Davies A, Berrow NS, Butcher AJ, Page KM & Dolphin AC (2001). Evidence for two concentration-dependent processes for β subunit effects on α1B calcium channels. *Biophys J* **81**, 1439–1451.

Catterall WA (2000). Structure and regulation of voltage-gated Ca^{2+} channels. *Annu Rev Cell Dev Biol* **16**, 521–555.

Chen YH, Li MH, Zhang Y, He LL, Yamada Y, Fitzmaurice A, Shen Y, Zhang H, Tong L & Yang J (2004). Structural basis of the α1–β subunit interaction of voltage-gated Ca^{2+} channels. *Nature* **429**, 675–680.

De Waard M, Scott VES, Pragnell M & Campbell KP (1996). Identification of critical amino acids involved in α_1–β interaction in voltage-dependent Ca^{2+} channels. *FEBS Lett* **380**, 272–276.

Dolphin AC (2003). β subunits of voltage-gated calcium channels. *J Bioenerg Biomembr* **35**, 599–620.

Gerster U, Neuhuber B, Groschner K, Striessnig J & Flucher BE (1999). Current modulation and membrane targeting of the calcium channel α_{1c} subunit are independent functions of the β subunit. *J Physiol* **517**, 353–368.

Hanlon MR, Berrow NS, Dolphin AC & Wallace BA (1999). Modelling of a voltage-dependent Ca^{2+} channel β subunit as a basis for understanding its functional properties. *FEBS Lett* **445**, 366–370.

Herlitze S, Garcia DE, Mackie K, Hille B, Scheuer T & Catterall WA (1996). Modulation of Ca^{2+} channels by G-protein $\beta\gamma$ subunits. *Nature* **380**, 258–262.

Ikeda SR (1996). Voltage-dependent modulation of N-type calcium channels by G protein $\beta\gamma$ subunits. *Nature* **380**, 255–258.

Leroy J, Richards MS, Butcher AJ, Nieto-Rostro M, Pratt WS, Davies A & Dolphin AC (2005). Interaction via a key tryptophan in the I–II linker of N-type calcium channels is required for β1 but not for palmitoylated β2, implicating an additional binding site in the regulation of channel voltage-dependent properties. *J Neurosci* **25**, 6984–6996.

Maltez JM, Nunziato DA, Kim J & Pitt GS (2005). Essential $Ca_v\beta$ modulatory properties are AID-independent. *Nat Struct Mol Biol* **12**, 372–377.

Meir A, Bell DC, Stephens GJ, Page KM & Dolphin AC (2000). Calcium channel β subunit promotes voltage-dependent modulation of α1B by $G\beta\gamma$. *Biophys J* **79**, 731–746.

Neely A, Wei X, Olcese R, Birnbaumer L & Stefani E (1993). Potentiation by the β subunit of the ratio of the ionic current to the charge movement in the cardiac calcium channel. *Science* **262**, 575–578.

Neuhuber B, Gerster U, Mitterdorfer J, Glossmann H & Flucher BE (1998). Differential effects of Ca^{2+} channel β_{1a} and β_{2a} subunits on complex formation with α_{1S} and on current expression in tsA201 cells. *J Biol Chem* **273**, 9110–9118.

Opatowsky Y, Chen CC, Campbell KP & Hirsch JA (2004). Structural analysis of the voltage-dependent calcium channel β subunit functional core and its complex with the α1 interaction domain. *Neuron* **42**, 387–399.

Pragnell M, De Waard M, Mori Y, Tanabe T, Snutch TP & Campbell KP (1994). Calcium channel β-subunit binds to a conserved motif in the I–II cytoplasmic linker of the α_1-subunit. *Nature* **368**, 67–70.

Raghib A, Bertaso F, Davies A, Page KM, Meir A, Bogdanov Y & Dolphin AC (2001). Dominant-negative synthesis suppression of voltage-gated calcium channel $Ca_v2.2$ induced by truncated constructs. *J Neurosci* **21**, 8495–8504.

Richards MW, Butcher AJ & Dolphin AC (2004). Calcium channel β-subunits: structural insights AID our understanding. *Trends Pharmacol Sci* **25**, 626–632.

Sandoz G, Lopez-Gonzalez I, Grunwald D, Bichet D, Altafaj X, Weiss N, Ronjat M, Dupuis A & De Waard M (2004). $Ca_v\beta$-subunit displacement is a key step to induce the reluctant state of P/Q calcium channels by direct G protein regulation. *Proc Natl Acad Sci U S A* **101**, 6267–6272.

Van Petegem F, Clark KA, Chatelain FC & Minor DL Jr (2004). Structure of a complex between a voltage-gated calcium channel β-subunit and an α-subunit domain. *Nature* **429**, 671–675.

Walker D & De Waard M (1998). Subunit interaction sites in voltage-dependent Ca^{2+} channels. *Trends Neurosci* **21**, 148–154.

Witcher DR, De Waard M, Liu H, Pragnell M & Campbell KP (1995). Association of native Ca^{2+} channel β subunits with the α_1 subunit interaction domain. *J Biol Chem* **270**, 18088–18093.

Zamponi GW & Snutch TP (1998). Decay of prepulse facilitation of N type calcium channels during G protein inhibition is consistent with binding of a single $G_{\beta\gamma}$ subunit. *Proc Natl Acad Sci U S A* **95**, 4035–4039.

Acknowledgements

This work was supported by The Wellcome Trust. We thank the following for generous gifts of cDNAs: Dr Y. Mori (Seriken, Okazaki, Japan) for rabbit $Ca_V2.2$; Dr M. Rees (University College London) for mouse $\alpha2\delta$-2; Dr E. Perez-Reyes (Loyola University, Chicago, IL, USA) for rat β2a; Professor P. G. Strange (Reading, UK) for rat D_2 dopamine receptor; Dr T. Hughes (Yale, New Haven, CT, USA) for mut-3 GFP and Genetics Institute (Cambridge, MA, USA) for pMT_2. We thank Dr K. Page for critical reading of this manuscript. We also thank K. Chaggar and L. Douglas for technical assistance.

Author's present address

J. Leroy: Inserm U-446, Laboratoire de Cardiologie Cellulaire et Moleculaire, Faculté de Pharmacie, Université Paris-Sud, 5, Rue J.-B. Clement, F-92296 Chatenay-Malabry cedex, France.

The importance of occupancy rather than affinity of CaVß subunits for the calcium channel I–II linker in relation to calcium channel function

Adrian J. Butcher, Jérôme Leroy, Mark W. Richards, Wendy S. Pratt and Annette C. Dolphin

J. Physiol. 2006;574;387-398; originally published online Apr 20, 2006;

DOI: 10.1113/jphysiol.2006.109744